Machine learning defined diagnostic criteria for differentiating pituitary metastasis from autoimmune hypophysitis in patients undergoing immune checkpoint blockade therapy

Ahmed Mekki, Laurent Dercle, Philip Lichtenstein, Ghaida Nasser, Aurélien Marabelle, Stéphane Champiat, Emilie Chouzenoux, Corinne Balleyguier, Samy Ammari

Machine-learning defined diagnostic criteria for differentiating pituitary metastasis from autoimmune hypophysitis in patients undergoing immune checkpoint blockade therapy

RUNNING TITLE

Diagnosis of autoimmune hypophysitis

AUTHORS

Ahmed MEKKI[1,2] ; Laurent DERCLE[3,4,] ; Philip LICHTENSTEIN[4] ; Ghaida NASSER[2]; Aurélien MARABELLE[5] ; Stéphane CHAMPIAT[5] ; Emilie CHOUZENOUX[6] ; Corinne BALLEYGUIER[1] ; Samy AMMARI[1]

1. Department of Radiology, Gustave Roussy Cancer Campus, Villejuif, France; Université Paris-Saclay, Paris, France. Electronic address: ahmekki@gmail.com
2. Department of neuroradiology, C.H.U Bicêtre AP-HP, Le Kremlin-Bicêtre, France
3. Université Paris-Saclay, Paris, France; Gustave Roussy, Université Paris-Saclay, Institut National de la Santé et de la Recherche Médicale (INSERM), U1015, Equipe Labellisée Ligue Nationale Contre le Cancer, Villejuif, F-94805, France.
4. Department of radiology, Columbia University Medical Center, NYC, NY
5. Drug Development Department, Gustave Roussy, Villejuif, France
6. Center for Visual Computing, CentraleSupelec, INRIA Saclay, 91190, Gif-sur-Yvette, France

CORRESPONDING AUTHOR

Laurent Dercle

laurent.dercle@gmail.com

+1 (917) 283 0908

UMR1015, Université Paris Saclay, Gustave Roussy, Villejuif, France

Department of Radiology, New York Presbyterian Hospital, Columbia University Medical Center, New York, New York, USA

ABSTRACT

Purpose:

New-onset pituitary gland lesions are observed in up to 18% of cancer patients undergoing treatment with immune checkpoint blockade (ICB) therapy. We aimed to develop and validate an imaging-based decision-making algorithm for use by the clinician that helps differentiate pituitary metastases from ICB-induced autoimmune hypophysitis.

Materials and Methods:

A systematic search was performed in the MEDLINE and EMBASE databases up to October 2018 to identify studies concerning immune-related hypophysitis (HP) in patients treated with CTLA-4 and PD(L)1, and pituitary metastasis (PM). The reference standard for diagnosis was confirmation by histology or response on follow-up imaging. Patients from included studies were randomly assigned to the training set or the validation set. Using machine learning (random forest tree algorithm) with the most-described 6 imaging and 3 clinical features, a multivariable prediction model (the signature) was developed and validated for diagnosing PM. Signature performance was evaluated using AUCs.

Results:

Out of 3,174 screened articles, 65 were included totalizing 122 patients (HP: 60 pts, PM: 62 pts). Complete radiological data were available in 82 pts (T: 62 pts, V: 20 pts). The signature reached an AUC=0.91 (0.82, 1.00), $P<10^{-8}$ in the training set and AUC=0.94 (0.80, 1.00), P=0.001 in the validation set. The signature predicted PM in lesions either ≥ 2cm in size or < 2cm if associated with heterogeneous contrast enhancement and cavernous extension.

Conclusion:

An image-based signature was developed with machine-learning and validated for differentiating PM from HP. This tool could be used by clinicians for enhanced decision-making in cancer patients undergoing ICB treatment with new-onset, concerning lesions of the pituitary gland.

KEYWORDS

CTLA-4; PD-1; PD-L1; immune related adverse events; hypophisitis; machine-learning

INTRODUCTION

Immune checkpoint blockers (ICB) primarily function by targeting the immunoinhibitory Cytotoxic T–Lymphocyte Associated Protein 4 (CTLA-4), Programmed Cell Death 1 (PD-1), and Programmed Cell Death Ligand (PD-L1). These medications have revolutionized the therapeutic landscape across many solid tumors (1–3). Their superiority over reference treatments was first demonstrated in melanoma (4,5) and have since expanded on to treat numerous other cancer types (6–10). The importance of these new anti-cancer treatments is attested to by their registration as a 'breakthrough therapy'; they are now a standard of care in many cancer types and are under therapeutic trial for many others (11). As a result, their use is no longer limited to the hospitals involved in clinical trials and they are prescribed in a much wider range of clinical oncology settings across the world. The number of patients exposed to these new therapies is likely to dramatically increase in the near future.

These new immunotherapies, however, bring new challenges for the oncologist. They generate atypical patterns of tumor responses and progression (12–16) as well as unique toxicity profiles (17). The recognition and management of immune related adverse-events (irAEs) poses new difficulties in particular for imaging physicians. Although still primordial, medical imaging is a cornerstone in the monitoring of patients undergoing ICB therapy. A previous study exploring this fundamental role showed a 74% imaging-based detection rate of anti-PD1 mediated irAEs (18) with the most frequent complications including interstitial lung disease, thoracic sarcoid-like reaction, thyroiditis, hypophysitis, enterocolitis, pancreatitis, hepatitis, arthritis, and tenosynovitis.

Hypophysitis (HP) is a well-known endocrinopathy in patients undergoing ICB therapy. The development of immune related hypophysitis has been more frequently observed with the anti-CTLA-4 agent ipilimumab (19–21) due to the expression of CTLA-4 on normal pituitary cells (22). Its incidence varies between 0.5% and 18% in a recent review (23), and is dose-dependent. When ipilimumab is given in combination with the anti-PD-1 agent nivolumab, the incidence of HP is around 8% (24). In contrast, HP is less frequent in patients treated with anti-PD-1 or anti-PD-L1 monotherapy (25).

The real difficulty in managing HP however comes not from the treatment itself but rather its accurate recognition and differentiation from pituitary metastasis (PM). An uncommon presentation outside of specialized centers, PM rises much higher on the differential for the physician working at a comprehensive cancer center. One of the largest historical series examined 500 consecutive autopsies in patients with metastatic disease at Memorial Sloan-Kettering Cancer Center and found an incidence of 3.6% (26), a number which may be set to rise as patients with malignancy continue to live longer and be monitored more closely.

The appearance of a focal anomaly in the pituitary gland of patients undergoing ICB therapy for malignancy poses a continued dilemma for the imaging physician, and one that comes up regularly at multidisciplinary meetings. The distinction between HP and PM is one that needs to be made quickly to avoid a potentially devastating delay in management. Clinico-biological data is not very discriminating, and histological confirmation requires invasive neurosurgical management. The place of medical imaging is therefore central in differentiating these two pathologies. In cases where the imaging appearance is equivocal and the diagnosis remains uncertain, however, a few options exist.

The “wait and see” strategy consists mainly of empiric treatment with corticosteroids when there is a strong HP presumption. This strategy carries the main advantage of non-invasiveness, but also the obvious risk of potentially missing the start of a rapidly progressive metastasis. This in turn risks irreversible damage to the visual pathways and a significantly more difficult neurosurgical management. It can also be a source of anxiety in patients with partial or complete response to these treatments. Proceeding with transphenoidal neurosurgical treatment in cases of uncertainty will protect the visual pathways and is most advantageous when the lesion is indeed metastatic, but there can be significant morbidity associated with inadvertently resecting an inflamed but otherwise normal pituitary. A third option consisting of treatment with probabilistic radiotherapy also risks permanent damage to the visual pathways in addition to irreversible hypopituitarism, radionecrosis, and damage to the internal carotid arteries.

To date, multiple case reports and series have been published describing ICB-related HP as well as PM, but there is no study comparing these 2 pathologies. Our objective was to assess whether an image-guided decision making algorithm can enable the non-invasive diagnosis of suspicious pituitary lesions in patients treated by these new anti-cancer immunotherapies. For this purpose we have performed a systematic review of literature with the aim of making a machine learning driven algorithm.

METHODS

Search methods

A systematic review of the literature was conducted according to the guidelines outlined in the Preferred Reporting Items for Systematic Reviews and Meta-Analyses (PRISMA) statement (27). The PUBMED and EMBASE databases were searched up to October 20, 2018. For HP, the search method involved querying for the terms “hypophysitis”, “auto-immune hypophysitis”, “ipilimumab”, “nivolumab”, “pembrolizumab”, “atezolizumab”, “cytotoxic T-lymphocyte antigen 4”, “CTLA-4”, “programmed cell death 1”, “PD-1”, “programmed cell death ligand 1”, “PD-L1”, “immunotherapy”, “checkpoint inhibitor”, “anti-PD-1”, “anti-PD-L1”, “anti-CTLA-4”. The Boolean operator AND was used to combine terms related to HP and ICB. The Boolean operator OR was used to discriminate the similar terms. For PM, the search method involved querying for the terms “pituitary metastasis”, “metastatic cancer of the pituitary”, “metastatic carcinoma of the pituitary”, “metastasis” and “pituitary”. No starting point was defined for article screening.

Inclusion criteria

For study selection, all search hits were evaluated for eligibility by two reviewers screening title and abstracts. Full-text versions of potentially eligible articles were obtained for further evaluation. The reference lists of the included studies were manually searched to identify other potentially eligible articles. Disagreements between the two reviewers in study selection were resolved by consulting a third reviewer (A.M, S.A. L.D.; radiologists with respectively 4, 10 and 8 years of experience).

Inclusion criteria were: (i) articles describing either HP or PM with at least 3 'standard' radiological signs (defined as any discriminating radiological sign used in more than 50% of the articles included), (ii) a diagnosis of HP confirmed by regression of the lesion with corticotherapy and/or the reduction or cessation of ICB therapy, (iii) a diagnosis of PM either confirmed histologically or by a non-equivocal metastatic progression on subsequent imaging.

Exclusion criteria were: (i) studies that were not published in English, (ii) animal studies, (iii) articles with magnetic resonance imaging that was too old or insufficient quality for our evaluation, (iv) association with a pituitary adenoma, meningioma, or primary carcinoma of pituitary.

Data extraction and analysis

Imaging signs were defined based on the international radiological pituitary reference book (28), on our expertise in oncological neuroimaging, and on the features most frequently cited in the included articles. First, we recorded all signs available in the selected studies. Second, we considered signs which were evaluated in more than 50% of the included articles as a relevant radiological sign; the remainder were deemed irrelevant and excluded. Third, in the event of insufficient radiological data (less than 3 relevant 'standard' radiological signs in a patient), the corresponding author was contacted by email to obtain the necessary radiological information. Fourth, in the absence of feedback from the corresponding author, two radiologists (A.M., S.A.) reinterpreted the available images with missing

radiological features without knowledge of outcome, clinical data, or clinico-pathological features. These data are hierarchized in Table 1a for PM and Table 1b for HP.

Development and validation of the signature in the training set

Performance of the clinical features, radiological features, and of the signature

The primary endpoint of this study was to train and validate a signature incorporating both clinical and radiological features to diagnose pituitary metastases. The secondary endpoint was to compare the accuracy (95CI) of (i) clinical features, (ii) radiological features, and (iii) the signature.

Predictors included in the signature

All relevant clinical and imaging variables (see above) were evaluated for their efficacy in predicting whether the pituitary lesion represented either a pituitary metastasis or an autoimmune hypophysitis.

Candidate Signature Building

Patients were randomly assigned to either the training set or the validation set using a ratio of 3:1. Patients with incomplete relevant clinical or radiological datasets were excluded from the training and validation of the signature. We developed (training set) and validated (validation set) a multivariable prediction model, *i.e*. the signature, to diagnose pituitary metastases based on all predictors in the training set. Specifically, the signature outputs the probability of a pituitary lesion being a metastasis. Patients with signature value > 0.5 were classified as positive for high-risk of metastasis, and negative/low-risk otherwise. First, AUC and ROC curves were used to rank non-redundant candidate features. To reduce overfitting, a maximum combination of three informative candidate features was selected based on forward search and feature combination. A random forest tree machine learning algorithm (CRT with pruning and 3-fold cross validation) was used to combine features and generate the optimal candidate classification model, *i.e*. the signature, that achieved the best performance in terms of area under a receiver operating characteristic curve (AUC) which was estimated by three-fold cross-validation.

Validation of the signature

The performance of the optimal signature was tested in the validation set containing patients that were never used for training. There was no difference between development dataset and validation dataset in terms of setting, eligibility criteria, outcome, and predictors. In cases of missing data, patients were excluded from the signature building.

Statistical analysis

Data were presented as frequency with percentages for qualitative variables and as mean with standard deviation for continuous variables. Calculated data with p values < 0.05 were considered as

statistically significant. The performance of the machine-learning algorithm for diagnosing pituitary metastases was calculated using a binary classifier system (pituitary metastases vs. immune-related hypophysitis) and nonparametric receiver operating characteristic curve (AUC). All statistical analyses were performed using SPSS software 24.0 (IBM, Armonk, New York). AUC comparisons for correlated ROC curves were performed using Hanley and McNeil techniques.

RESULTS

Search strategy and study selection

The systematic review through MEDLINE and PUBMED databases yielded 3,174 records that met the initial search criteria. *Figure 1* outlines the prisma consort flow, duplicates, and excluded articles. Ultimately, 65 articles were included of which there were 49 case reports and 16 case series; 25 were in the HP group (18, 29–52) and 40 were in the PM group (53–92). This yielded a total of 122 patients (60 in the HP group and 62 in the PM group) included for 'standard' radiological sign determination. Of these, a further 40 patients were excluded from signature building due to insufficient total radiological data.

Patients' characteristics

Table 1 summarizes the patient demographics. The mean age of the patient cohort was 56.9 ± 12 years, with range of 23-87 years old. Of the 121 patients whose gender was known, 55 patients (45.5%) were female and 66 (55.5%) were male.

Imaging signs selection

Amongst a total of 16 imaging signs that were used in these 122 patients, 8 were evaluated in more than 50% of the literature and considered as 'standard' radiological signs. The eight 'standard' radiological signs (with % citation and description variables) were: pituitary gland enlargement (99.2%, n=121/122pts, enlarged vs. not enlarged), contrast enhancement (77.9%, n=95/122pts, homogenous vs. heterogeneous), pituitary stalk thickness (87%, n=107/122pts, increased vs. normal), cavernous extension (98.4%, n=120/122pts, presence vs. absence), suprasellar extension (99%, n=121/122pts, presence vs. absence), and size (98.4%, n=120/122 pts, increased vs. normal (increased size was a continuous variable that we then empirically divided into 2 categories: $\geq$ 2cm vs. $<$ 2cm)). 18FDG PET uptake was also included because of its systematic use in the articles of nuclear medicine (100.0%, n=4/4 pts, normal vs. increased). Eight non 'standard' radiological signs were excluded from our analysis: T1 signal, T2 signal, diffusion signal, posterior lobe signal, lesion epicenter, pituitary stalk deviation, chiasma anomaly, and peridural enhancement. All of these signs were reported in less than 10% of the manuscript from the literature.

Performance of the signature

Complete radiological data were available in 82 pts (Training: 62 pts, Validation: 20 pts). The signature reached an AUC=0.91 (0.82, 1.00), $P<10^{-8}$ in the training set and AUC=0.94 (0.80, 1.00), P=0.001 in the validation set (Figure 4). The signature predicted a PM in patients that had either a pituitary lesion $\geq$ 2cm in size or a lesion $<$ 2cm that also demonstrated both heterogeneous contrast enhancement and cavernous extension (Figure 3). *Table 3* summarizes the sensitivity, specificity,

positive predictive value, and negative predictive value of all modalities. The signature of size ≥ 2cm was most superior in its specificity; a positive finding was observed exclusively in cases of PM (100%; Training: 22/22 pts, Validation: 16/16 pts).

For lesions < 2cm, the algorithm found that a heterogeneously enhancing lesion associated with cavernous extension was PM 100% of the time. The algorithm suggests HP for lesions that are less than < 2cm that either enhance heterogeneously without cavernous extension or enhance homogenously. The categories can be broken down as follows: (i) Size < 2cm and homogeneous enhancement (T: 3.3%, V:28.0%); (ii) Size < 2cm and heterogeneous enhancement without cavernous extension (T:40%, V:16.7%); (iii) Size < 2cm and heterogeneous enhancement with cavernous extension (T:100%, V:Not Evaluable); (iv) Size ≥ 2cm (T: 100%, V:100%)

Immune-related hypophysitis characteristics

Figure 2a-c shows examples of immune-related hypophysitis and *Table 2* summarizes immune-related hypophysitis disease characteristics by patient. Homogenous enhancement was observed in 63.3% (n=31/49pts) and size was never ≥ 2cm (n=0/59pts). The median time of immune-related hypophysitis occurrence was 10 weeks (range 3–56 weeks). An objective response to immunotherapy was observed in 56% of patients (n=14/25pts), partial response was seen in 40% (n=10/25pts), complete response in 16% (n=4/25pts), progressive disease in 24% (n=6/25pts), and stable disease in 20% (n=5/25pts).

Pituitary metastases characteristics

Figure 2d-f shows examples of pituitary metastases and *Table 2* summarizes disease characteristics by patient. Heterogenous enhancement was observed in 82.6% (n=38/46pts) and a size ≥ 2cm in 67.2% (n=45/61pts). Primary tumor type was breast in 23% (n=14/61pts), NSCLC in 18% (n=11/61pts), RCC in 16.4% (n=10/61pts), thyroid in 13.1% (n=8/61pts), HCC in 4.9% (3/61pts), SCLC in 3.3% (n=2/61pts), melanoma in 3.3% (n=2/61pts), and other cancer types in 18% (n=11/61pts).

DISCUSSION

This systematic review of the literature allows us to more accurately characterize the appearance of focal anomalies of the pituitary gland in patients undergoing ICB therapy and differentiate between metastatic progression and an immune related adverse event. A radiologic signature achieving the best performance in diagnosing PM was determined using a machine learning-based multivariable prediction model. Additionally, a new methodology was implemented to perform data mining in the existing literature and identify the largest existing cohort of PM and HP. The 2 most discriminating signs discovered were size ≥ 2cm and cavernous extension.

The frequency of immune-related HP can reach up to 18% (93), occurs mainly in patients who are responding to immunotherapy, and typically appears around 10 weeks after the initiation of treatment. This 10-week delay is a median value with the literature showing a very wide range from 1 to 52 weeks (94). Although our data mining allowed us to characterize the typical clinic-biological profile of these patients, none of these features were selected by the model. Patients with HP commonly presented with headache and pituitary insufficiency, but rarely with diabetes insipidus. The signs and symptoms at diagnosis as well as the pituitary hormone abnormalities largely depend on the degree of pituitary involvement. PM in our review demonstrated the same clinical presentation as HP aside from a higher frequency of diabetes insipidus.

We have seen that the radiological appearance of immune-related hypophysitis secondary to ICB therapy is similar to that described in primary hypophysitis (28) with diffuse and symmetric enlargement of the pituitary gland as well as frequent suprasellar extension, pituitary stalk thickening, and homogenous enhancement. Pituitary metastases also demonstrated enlargement of the pituitary gland, but these often exceeded 2cm in maximal diameter with frequently extended into the cavernous sinuses (neither of these features were seen in our cohort of HP). An intense, heterogeneous pattern of enhancement also favored the diagnosis of metastasis.

An important limitation to note is that we've only evaluated the imaging of acute phase HP, when the problem of differentiating from PM is at its greatest. Imaging of the late phase of HP typically poses less of a dilemma as atrophy of the anterior pituitary is common. Moreover, we did not include in our analysis the possibility of pituitary adenoma given the fact that patients will usually have baseline brain imaging and the occurrence of new pituitary adenomas in an oncological context is unlikely. Finally, several radiological signs commonly used in the evaluation of pituitary pathology were not included in our analysis because of their low quotation in the included articles.

We chose meta-analysis because it was the only way to collect enough data with a diagnosis of certainty. For patients with PM, we did not take into account the individual anti-oncologic treatments for two reasons: scarce data is available for PM in patients undergoing ICB therapy, and based on our experience we do not believe that the imaging appearance of PM differs significantly across treatment types. Additionally, we have prospectively tested our algorithm on 3 patients at our institutions that presented with new pituitary lesions after ICB initiation, and a correct classification was observed for all (2 HP, 1PM) after a follow-up of 6 weeks.

The radiologist plays a crucial role in the care of patients treated with ICB and the evaluation of response to treatment is a great challenge in the context of atypical patterns of response and progression with drugs targeting the immune environment. The radiologist faces new pituitary lesions, whether it be on routine oncological follow-up imaging or the targeted investigation of new headaches, ante-pituitary insufficiency, or diabetes insipidus. Misinterpretation of the appearance and therefore pathology can yield vastly different treatment pathways and potentially expose the patient to significant morbidity that might have otherwise been avoided. Symptomatic HP for instance may be treated with corticosteroids and temporary suspension of the ICB (15), while a suspected PM may lead to a change of therapeutic regimen, neurosurgical intervention, or radiotherapy. Our imaging-based decisional algorithm aims to help both radiologists and oncologists make the right diagnosis for early and optimized management of pituitary anomalies in the growing population of patients undergoing immunotherapy.

Conflicts of interest

None

REFERENCES

1. Keir ME, Butte MJ, Freeman GJ, Sharpe AH. PD-1 and Its Ligands in Tolerance and Immunity. Annu Rev Immunol. 2008;26(1):677–704.

2. Peggs KS, Quezada SA, Korman AJ, Allison JP. Principles and use of anti-CTLA4 antibody in human cancer immunotherapy. Curr Opin Immunol. 2006;18(2):206–213.

3. LaBeck NM, Jean GW, Huynh C, Alzghari SK, Lowe DB. Immune Checkpoint Inhibitors: New Insights and Current Place in Cancer Therapy. Pharmacother J Hum Pharmacol Drug Ther. 2015;35(10):963–976.

4. Robert C, Long GV, Brady B, et al. Nivolumab in Previously Untreated Melanoma without BRAF Mutation. N Engl J Med. 2015;372(4):320–330.

5. Hodi FS, O'Day SJ, McDermott DF, et al. Improved Survival with Ipilimumab in Patients with Metastatic Melanoma. N Engl J Med. 2010;363(8):711–723.

6. Brahmer J, Reckamp KL, Baas P, et al. Nivolumab versus Docetaxel in Advanced Squamous-Cell Non-Small-Cell Lung Cancer. N Engl J Med. 2015;373(2):123–135.

7. Garon EB, Rizvi NA, Hui R, et al. Pembrolizumab for the Treatment of Non–Small-Cell Lung Cancer. N Engl J Med. 2015;372(21):2018–2028.

8. Motzer RJ, Escudier B, McDermott DF, et al. Nivolumab versus Everolimus in Advanced Renal Cell Carcinoma. N Engl J Med. 2015;373(19):1803–1813.

9. Bilgin B, Sendur MAN, Akıncı MB, Dede DŞ, Yalçın B. Targeting the PD-1 pathway: a new hope for gastrointestinal cancers. Curr Med Res Opin. 2017;33(4):749–759.

10. Ferris RL, Blumenschein G, Fayette J, et al. Nivolumab for Recurrent Squamous-Cell Carcinoma of the Head and Neck. N Engl J Med. 2016;375(19):1856–1867.

11. Tang J, Yu JX, Hubbard-Lucey VM, Neftelinov ST, Hodge JP, Lin Y. Trial watch: The clinical trial landscape for PD1/PDL1 immune checkpoint inhibitors. Nat Rev Drug Discov. 2018;17:854–855.

12. Dercle L, Seban R-D, Lazarovici J, et al. 18F-FDG PET and CT Scans Detect New Imaging Patterns of Response and Progression in Patients with Hodgkin Lymphoma Treated by Anti–Programmed Death 1 Immune Checkpoint Inhibitor. J Nucl Med. 2018;59(1):15–24.

13. Dercle L, Ammari S, Seban R-D, et al. Kinetics and nadir of responses to immune checkpoint blockade by anti-PD1 in patients with classical Hodgkin lymphoma. Eur J Cancer. 2018;91:136–144.

14. Turpin A, Michot J-M, Kempf E, et al. Le lymphome de Hodgkin : stratégies thérapeutiques actuelles et futures. Bull Cancer (Paris). 2018;105(1):81–98.

15. Champiat S, Lambotte O, Barreau E, et al. Management of immune checkpoint blockade dysimmune toxicities: a collaborative position paper. Ann Oncol. 2016;27(4):559–574.

16. Michot J-M, Mazeron R, Dercle L, et al. Abscopal effect in a Hodgkin lymphoma patient treated by an anti-programmed death 1 antibody. Eur J Cancer. 2016;66:91–94.

17. Weber JS, Hodi FS, Wolchok JD, et al. Safety Profile of Nivolumab Monotherapy: A Pooled Analysis of Patients With Advanced Melanoma. J Clin Oncol. 2016;35(7):785–792.

18. Mekki A, Dercle L, Lichtenstein P, et al. Detection of immune-related adverse events by medical imaging in patients treated with anti-programmed cell death 1. Eur J Cancer. 2018;96:91–104.

19. Kwak JJ, Tirumani SH, Van den Abbeele AD, Koo PJ, Jacene HA. Cancer Immunotherapy: Imaging Assessment of Novel Treatment Response Patterns and Immune-related Adverse Events. RadioGraphics. 2015;35(2):424–437.

20. Haanen JB a. G, Carbonnel F, Robert C, et al. Management of toxicities from immunotherapy: ESMO Clinical Practice Guidelines for diagnosis, treatment and follow-up. Ann Oncol. 2018;29(Supplement_4):iv264-iv266.

21. Cukier P, Santini FC, Scaranti M, Hoff AO. Endocrine side effects of cancer immunotherapy. Endocr Relat Cancer. 2017;24(12):T331–T347.

22. Iwama S, Remigis AD, Callahan MK, Slovin SF, Wolchok JD, Caturegli P. Pituitary Expression of CTLA-4 Mediates Hypophysitis Secondary to Administration of CTLA-4 Blocking Antibody. Sci Transl Med. 2014;6(230):230ra45-230ra45.

23. Solinas C, Porcu M, De Silva P, et al. Cancer immunotherapy-associated hypophysitis. Semin Oncol. 2018;45(3):181–186.

24. Larkin J, Chiarion-Sileni V, Gonzalez R, et al. Combined Nivolumab and Ipilimumab or Monotherapy in Untreated Melanoma. N Engl J Med. 2015;373(1):23–34.

25. Weber J, Mandala M, Del Vecchio M, et al. Adjuvant Nivolumab versus Ipilimumab in Resected Stage III or IV Melanoma. N Engl J Med. 2017;377(19):1824–1835.

26. Max MB, Deck MDF, Rottenberg DA. Pituitary metastasis: Incidence in cancer patients and clinical differentiation from pituitary adenoma. Neurology. 1981;31(8):998–998.

27. Shamseer L, Moher D, Clarke M, et al. Preferred reporting items for systematic review and meta-analysis protocols (PRISMA-P) 2015: elaboration and explanation. BMJ. 2015;349:g7647.

28. Bonneville J-F, Bonneville F, Cattin F, Nagi S. MRI of the Pituitary Gland. Springer International Publishing; 2016.//www.springer.com/gp/book/9783319290416. Accessed October 26, 2018.

29. Cheema A. Ipilimumab-induced secondary hypophysitis. Endocr Pract. 2018;24(9):854–854.

30. Hiel B van der, Blank CU, Haanen JB a g, Stokkel MP m. Detection of Early Onset of Hypophysitis by 18f-fdg Pet-ct in a Patient With Advanced Stage Melanoma Treated With Ipilimumab. Clin Nucl Med. 2013;38(4)https://insights.ovid.com/pubmed?pmid=23455528. Accessed November 4, 2018.

31. Blansfield JA, Beck KE, Tran K, et al. Cytotoxic T-Lymphocyte–Associated Antigen-4 Blockage Can Induce Autoimmune Hypophysitis in Patients With Metastatic Melanoma and Renal Cancer. J Immunother Hagerstown Md 1997. 2005;28(6):593–598.

32. Albarel F, Gaudy C, Castinetti F, et al. Long-term follow-up of ipilimumab-induced hypophysitis, a common adverse event of the anti-CTLA-4 antibody in melanoma. Eur J Endocrinol. 2015;172(2):195–204.

33. Araujo PB, Coelho MCA, Arruda M, Gadelha MR, Neto LV. Ipilimumab-induced hypophysitis: review of the literature. J Endocrinol Invest. 2015;38(11):1159–1166.

34. Carpenter KJ, Murtagh RD, Lilienfeld H, Weber J, Murtagh FR. Ipilimumab-Induced Hypophysitis: MR Imaging Findings. Am J Neuroradiol. 2009;30(9):1751–1753.

35. Chang L-S, Yialamas MA. Checkpoint Inhibitor-Associated Hypophysitis. J Gen Intern Med. 2018;33(1):125–127.

36. Chodakiewitz Y, Brown S, Boxerman JL, Brody JM, Rogg JM. Ipilimumab treatment associated pituitary hypophysitis: Clinical presentation and imaging diagnosis. Clin Neurol Neurosurg. 2014;125:125–130.

37. Dillard T, Yedinak CG, Alumkal J, Fleseriu M. Anti-CTLA-4 antibody therapy associated autoimmune hypophysitis: serious immune related adverse events across a spectrum of cancer subtypes. Pituitary. 2010;13(1):29–38.

38. Hassanzadeh B, DeSanto J, Kattah JC. Ipilimumab-induced Adenohypophysitis and Orbital Apex Syndrome: Importance of Early Diagnosis and Management. Neuro-Ophthalmol. 2017;42(3):176–181.

39. Johnson DB, Mudigonda TV, Sosman JA. Melanoma and a Headache. JAMA Oncol. 2015;1(8):1167–1168.

40. Juszczak A, Gupta A, Karavitaki N, Middleton MR, Grossman AB. MECHANISMS IN ENDOCRINOLOGY: Ipilimumab: a novel immunomodulating therapy causing autoimmune hypophysitis: a case report and review. Eur J Endocrinol. 2012;167(1):1–5.

41. Kaehler KC, Egberts F, Lorigan P, Hauschild A. Anti-ctla-4 therapy-related autoimmune hypophysitis in a melanoma patient. Melanoma Res. 2009;19(5):333–334.

42. Kanie K, Iguchi G, Bando H, et al. Two Cases of Atezolizumab-Induced Hypophysitis. J Endocr Soc. 2017;2(1):91–95.

43. Mahzari M, Liu D, Arnaout A, Lochnan H. Immune Checkpoint Inhibitor Therapy Associated Hypophysitis. Clin Med Insights Endocrinol Diabetes. 2015;8:21–28.

44. Majchel D, Korytkowski MT. Anticytotoxic T-Lymphocyte Antigen-4 Induced Autoimmune Hypophysitis: A Case Report and Literature Review. Case Rep. Endocrinol. 2015.https://www.hindawi.com/journals/crie/2015/570293/. Accessed November 4, 2018.

45. Marlier J, Cocquyt V, Brochez L, Van Belle S, Kruse V. Ipilimumab, not just another anti-cancer therapy: hypophysitis as side effect illustrated by four case-reports. Endocrine. 2014;47(3):878–883.

46. Gunawan F, George E, Roberts A. Combination immune checkpoint inhibitor therapy nivolumab and ipilimumab associated with multiple endocrinopathies. Endocrinol Diabetes Metab Case Rep. 2018;2018https://www.ncbi.nlm.nih.gov/pmc/articles/PMC5830856/.

47. Ohara N, Ohashi K, Fujisaki T, et al. Isolated Adrenocorticotropin Deficiency due to Nivolumab-induced Hypophysitis in a Patient with Advanced Lung Adenocarcinoma: A Case Report and Literature Review. Intern Med. 2018;57(4):527–535.

48. Okano Y, Satoh T, Horiguchi K, et al. Nivolumab-induced hypophysitis in a patient with advanced malignant melanoma. Endocr J. 2016;63(10):905–912.

49. Valecha G, Pant M, Ibrahim U, Atallah JP. Immunotherapy-induced autoimmune hypophysitis. J Oncol Pharm Pract. 2017;1078155217727142.

50. Wachsmann JW, Ganti R, Peng F. Immune-mediated Disease in Ipilimumab Immunotherapy of Melanoma with FDG PET-CT. Acad Radiol. 2017;24(1):111–115.

51. Wallace J, Krupa M, Brennan J, Mihlon F. Ipilimumab cystic hypophysitis mimicking metastatic melanoma. Radiol Case Rep. 2018;13(3):740–742.

52. Iqbal F, Choudhary N, Flanagan D. A case of pituitary hypophysitis following treatment with ipilimumab. BioScientifica; 2016.https://www.endocrine-abstracts.org/ea/0044/ea0044EP72. Accessed October 27, 2018.

53. Al-Aridi R, El Sibai K, Fu P, Khan M, Selman WR, Arafah BM. Clinical and biochemical characteristic features of metastatic cancer to the sella turcica: an analytical review. Pituitary. 2014;17(6):575–587.

54. Dutta P, Bhansali A, Shah VN, et al. Pituitary metastasis as a presenting manifestation of silent systemic malignancy: A retrospective analysis of four cases. Indian J Endocrinol Metab. 2011;15(Suppl3):S242–S245.

55. Bhatoe HS, Badwal S, Dutta V, Kannan N. Pituitary metastasis from medullary carcinoma of thyroid: case report and review of literature. J Neurooncol. 2008;89(1):63.

56. Ersoy R, Topaloglu O, Aydin C, Dirikoc A, Cakir B. Pituitary metastasis of breast cancer confirmed by fluorine-18 fluorodeoxyglucose positron emission tomography: A case report. J Endocrinol Invest. 2007;30(6):532–533.

57. Fridley J, Adams G, Rao V, et al. Small cell lung cancer metastasis in the pituitary gland presenting with seizures and headache. J Clin Neurosci. 2011;18(3):420–422.

58. Goglia U, Ferone D, Sidoti M, et al. Treatment of a pituitary metastasis from a neuroendocrine tumour: case report and literature review. Pituitary. 2008;11(1):93–102.

59. Gołkowski F, Trofimiuk M, Czepko R, et al. Two Rare Cases of Pituitary Metastases from Breast and Kidney Cancers. Exp Clin Endocrinol Diabetes. 2007;115(08):537–540.

60. Gopan T, Toms SA, Prayson RA, Suh JH, Hamrahian AH, Weil RJ. Symptomatic pituitary metastases from renal cell carcinoma. Pituitary. 2007;10(3):251–259.

61. He W, Chen F, Dalm B, Kirby PA, Greenlee JDW. Metastatic involvement of the pituitary gland: a systematic review with pooled individual patient data analysis. Pituitary. 2015;18(1):159–168.

62. Kam J, Kam J, Mann GB, et al. Solitary pituitary metastasis from HER2-positive breast cancer. Asia Pac J Clin Oncol. 2017;13(2):e181–e184.

63. Karamouzis MV, Melachrinou M, Fratzoglou M, Labropoulou-Karatza C, Kalofonos HP. Hepatocellular carcinoma metastasis in the pituitary gland: case report and review of the literature. J Neurooncol. 2003;63(2):173–177.

64. Ko J-C, Yang P-C, Huang T-S, Yeh K-H, Kuo S-H, Luh K-T. Panhypopituitarism Caused by Solitary Parasellar Metastasis From Lung Cancer. CHEST. 1994;105(3):951–953.

65. Koshiyama H, Ohgaki K, Hida S, et al. Metastatic renal cell carcinoma to the pituitary gland presenting with hypopituitarism. J Endocrinol Invest. 1992;15(9):677–681.

66. Lin E-Y, Hsieh C-T, Lin C-S, Tsai T-H, Chiang Y-H. Keyhole Surgery for Isolated Pituitary Stalk Metastatic Tumors: A Case Report and Review of the Literature. Min - Minim Invasive Neurosurg. 2008;51(04):222–224.

67. Masui K, Yonezawa T, Shinji Y, Nakano R, Miyamae S. Pituitary Apoplexy Caused by Hemorrhage From Pituitary Metastatic Melanoma: Case Report. Neurol Med Chir (Tokyo). 2013;53(10):695–698.

68. Ozturk MA, Eren OO, Sarikaya B, Aslan E, Oyan B. Pituitary Metastasis of Colon Adenocarcinoma: A Rare Occurrence. J Gastrointest Cancer. 2014;45(1):85–87.

69. Peppa M, Papaxoinis G, Xiros N, Hadjidakis D, Raptis SA, Economopoulos T. Panhypopituitarism due to Metastases to the Hypothalamus and the Pituitary Resulting From Primary Breast Cancer: A Case Report and Review of the Literature. Clin Breast Cancer. 2009;9(4):E4–E7.

70. Piedra MP, Brown PD, Carpenter PC, Link MJ. Resolution of diabetes insipidus following gamma knife surgery for a solitary metastasis to the pituitary stalk: Case report. J Neurosurg. 2004;101(6):1053–1056.

71. Riemenschneider MJ, Beseoglu K, Hänggi D, Reifenberger G. Prostate Adenocarcinoma Metastasis in the Pituitary Gland. Arch Neurol. 2009;66(8):1036–1036.

72. Siqueira PF de, Mathez ALG, Pedretti DB, et al. Pituitary metastasis of lung neuroendocrine carcinoma: case report and literature review. Arch Endocrinol Metab. 2015;59(6):548–553.

73. Williams MD, Asa SL, Fuller GN. Medullary thyroid carcinoma metastatic to the pituitary gland: an unusual site of metastasis. Ann Diagn Pathol. 2008;12(3):199–203.

74. Ratti M, Passalacqua R, Poli R, et al. Pituitary gland metastasis from rectal cancer: report of a case and literature review. SpringerPlus. 2013;2(1):467.

75. Stojanović M, Pekić S, Doknić M, et al. What's in the Image? Pituitary Metastasis from Papillary Carcinoma of the Thyroid: A Case Report and a Comprehensive Review of the Literature. Eur Thyroid J. 2013;1(4):277–284.

76. Beckett DJ, Gama R, Wright J, Ferns GAA. Renal Carcinoma Presenting with Adrenocortical Insufficiency Due to a Pituitary Metastasis. Ann Clin Biochem. 1998;35(4):542–544.

77. Moreno-Perez O, Peiró FM, López P, et al. An isolated pituitary metastasis as presentation of a differentiated hepatocellular carcinoma mimicking a non-functioning macroadenoma. J Endocrinol Invest. 2007;30(5):428–433.

78. Agarwal KK, Sharma P, Singla S, Kc SS, Bal C, Kumar R. A Rare Case of Non–small Cell Lung Cancer Metastasizing to the Pituitary Gland: Detection With 18f-fdg Pet-ct. Clin Nucl Med. 2014;39(5)https://insights.ovid.com/crossref?an=00003072-201405000-00028. Accessed November 4, 2018.

79. Barbaro D, Desogus N, Boni G. Pituitary metastasis of thyroid cancer. Endocrine. 2013;43(3):485–493.

80. Kurkjian C, Armor JF, Kamble R, Ozer H, Kharfan-Dabaja MA. Symptomatic metastases to the pituitary infundibulum resulting from primary breast cancer. Int J Clin Oncol. 2005;10(3):191–194.

81. Castle-Kirszbaum M, Goldschlager T, Ho B, Wang YY, King J. Twelve cases of pituitary metastasis: a case series and review of the literature. Pituitary. 2018;21(5):463–473.

82. Santarpia L, Gagel RF, Sherman SI, Sarlis NJ, Evans DB, Hoff AO. Diabetes insipidus and panhypopituitarism due to intrasellar metastasis from medullary thyroid cancer. Head Neck. 2009;31(3):419–423.

83. Wendel C, Campitiello M, Plastino F, et al. Pituitary Metastasis from Renal Cell Carcinoma: Description of a Case Report. Am J Case Rep. 2017;18:7–11.

84. Feletti A, Marton E, Rossi S, Canal F, Longatti P, Billeci D. Pituitary metastasis of Merkel cell carcinoma. J Neurooncol. 2010;97(2):295–299.

85. Kim YH, Lee B jun, Lee KJ, Cho JH. A Case of Pituitary Metastasis from Breast Cancer That Presented as Left Visual Disturbance. J Korean Neurosurg Soc. 2012;51(2):94–97.

86. Chu T-P, Tsai C-C, Chan W-C, Tzen C-Y, Chang Y-C. Solitary pituitary metastasis from breast cancer that presented as visual field defect. J Cancer Res Pract. 2016;3(4):140–143.

87. Kanayama S, Matsuno A, Nagashima T, Ishida Y. Symptomatic pituitary metastasis of malignant thymoma. J Clin Neurosci. 2005;12(8):953–956.

88. Mota JS, de Sá Caldas A, de Araújo Cortês Nascimento AGP, Faria M dos S, Sobral CSP. Pituitary Metastasis of Thyroid Carcinoma: A Case Report. Am J Case Rep. 2018;19:896–902.

89. Rajput R, Bhansali A, Dutta P, Gupta SK, Radotra BD, Bhadada S. Pituitary metastasis masquerading as non-functioning pituitary adenoma in a woman with adenocarcinoma lung. Pituitary. 2006;9(2):155–157.

90. Bišof V, Juretić A, Šarić N, et al. Pituitary metastasis of renal cell carcinoma : a case report. Radiol Oncol. 2009;42(4):225–231.

91. Hsiao C-H, Wang C-Y, Chung M-T, Yang M-S. Diabetes insipidus due to pituitary metastasis in a woman with lung adenocarcinoma: a case report. Cent Eur J Med. 2011;6(4):475–479.

92. Lim W, Lim DS, Chng CL, Lim AY. Thyroid Carcinoma with Pituitary Metastases: 2 Case Reports and Literature Review. Case Rep Endocrinol. 2015;2015https://www.ncbi.nlm.nih.gov/pmc/articles/PMC4320791/.

93. Eggermont AMM, Chiarion-Sileni V, Grob J-J, et al. Adjuvant ipilimumab versus placebo after complete resection of high-risk stage III melanoma (EORTC 18071): a randomised, double-blind, phase 3 trial. Lancet Oncol. 2015;16(5):522–530.

94. Prete A, Salvatori R. Hypophysitis. In: De Groot LJ, Chrousos G, Dungan K, et al., editors. Endotext. South Dartmouth (MA): MDText.com, Inc.; 2018.http://www.ncbi.nlm.nih.gov/books/NBK519842/.

TABLES AND FIGURES

Figure 1: **Study selection flowchart**

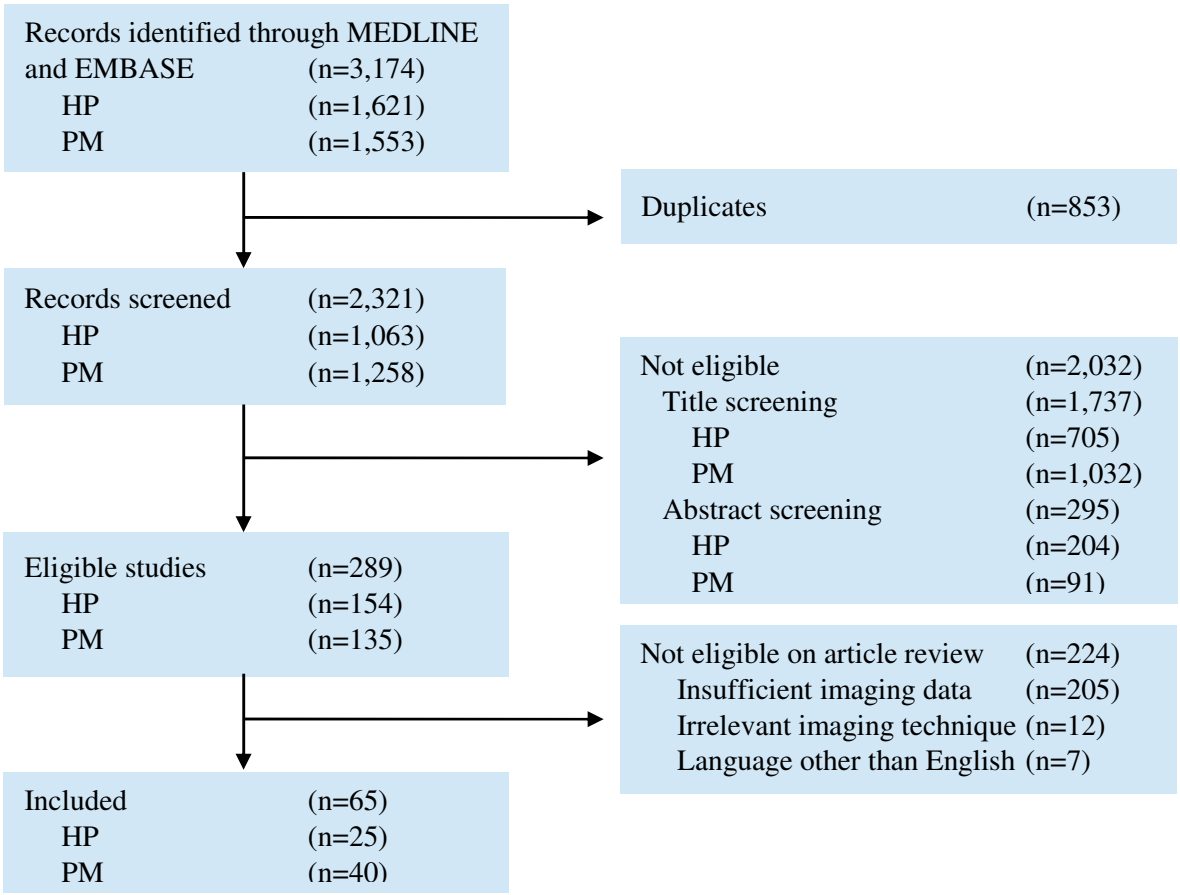

Figure 2: **Prospective evaluation of the image-driven algorithm**

ICB-induced hypophysitis (a-c) versus pituitary metastases (d-g) on oncological follow-up imaging (post-contrast T1-weighted MRI: sagittal (a, b, c and g), coronal (d and f), and axial (e)). All lesions were correctly predicted as HP or PM by our image-driven algorithm.

(a): Enlarged homogenously enhancing pituitary gland with a mildly thickened stalk. (b): Marked thickening of the pituitary stalk. (c): Enlarged pituitary (<2cm, no cavernous extension) with heterogenous enhancement. (d): Enlarged (≥ 2cm, with cavernous extension), heterogeneously enhancing pituitary gland in a patient treated for NSCLC. (e and f-g): Enlarged (<2cm, with cavernous extension), heterogeneously enhancing pituitary glands in 2 patients treated for RCC.

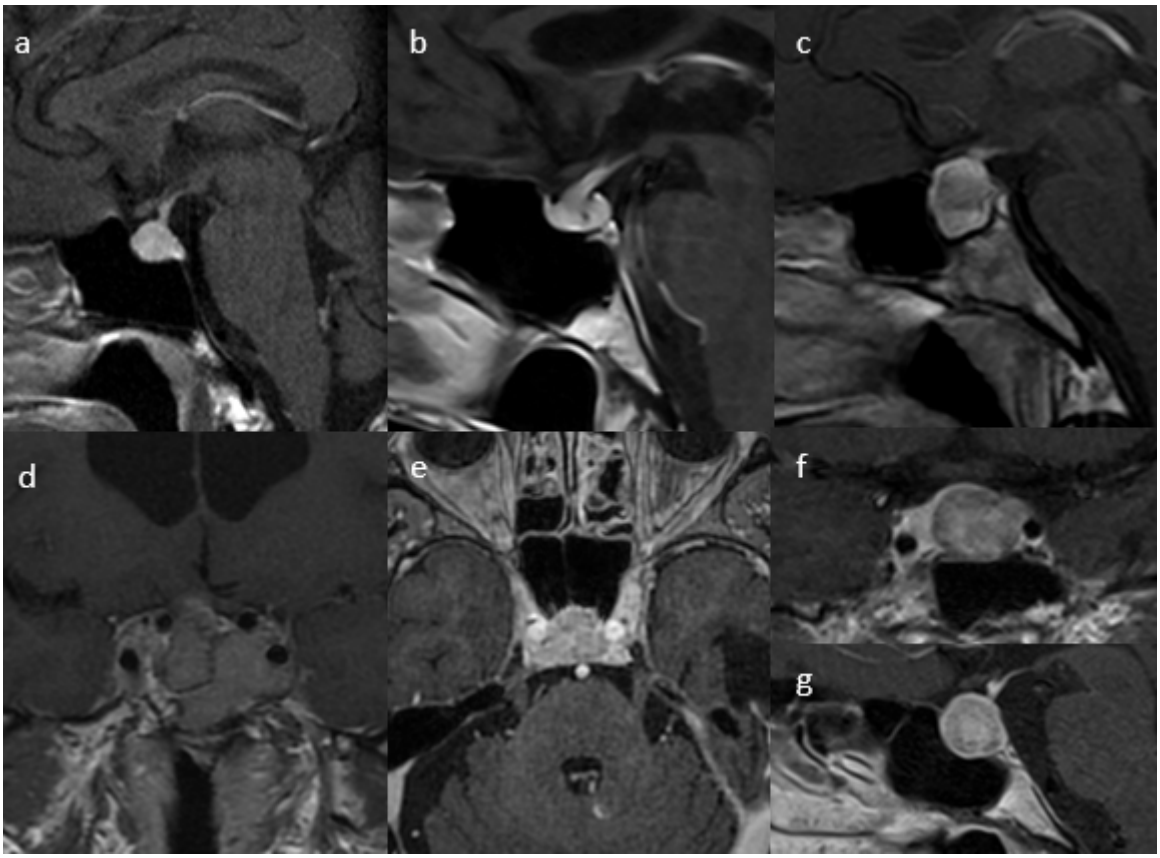

Figure 3: **Clinical decision algorithm trained (T) and validated (V) for the diagnosis of hypophysitis vs. pituitary metastases.**
Four categories were identified: (i) Size<2cm and homogeneous enhancement (T: 3.3%, V:28.0%); (ii) Size<2cm and heterogeneous enhancement without cavernous extension (T:40%, V:16.7%); (iii) Size<2cm and heterogeneous enhancement with cavernous extension (T:100%, V:NE); (iv) Size >2cm (T: 100%, V:100%)

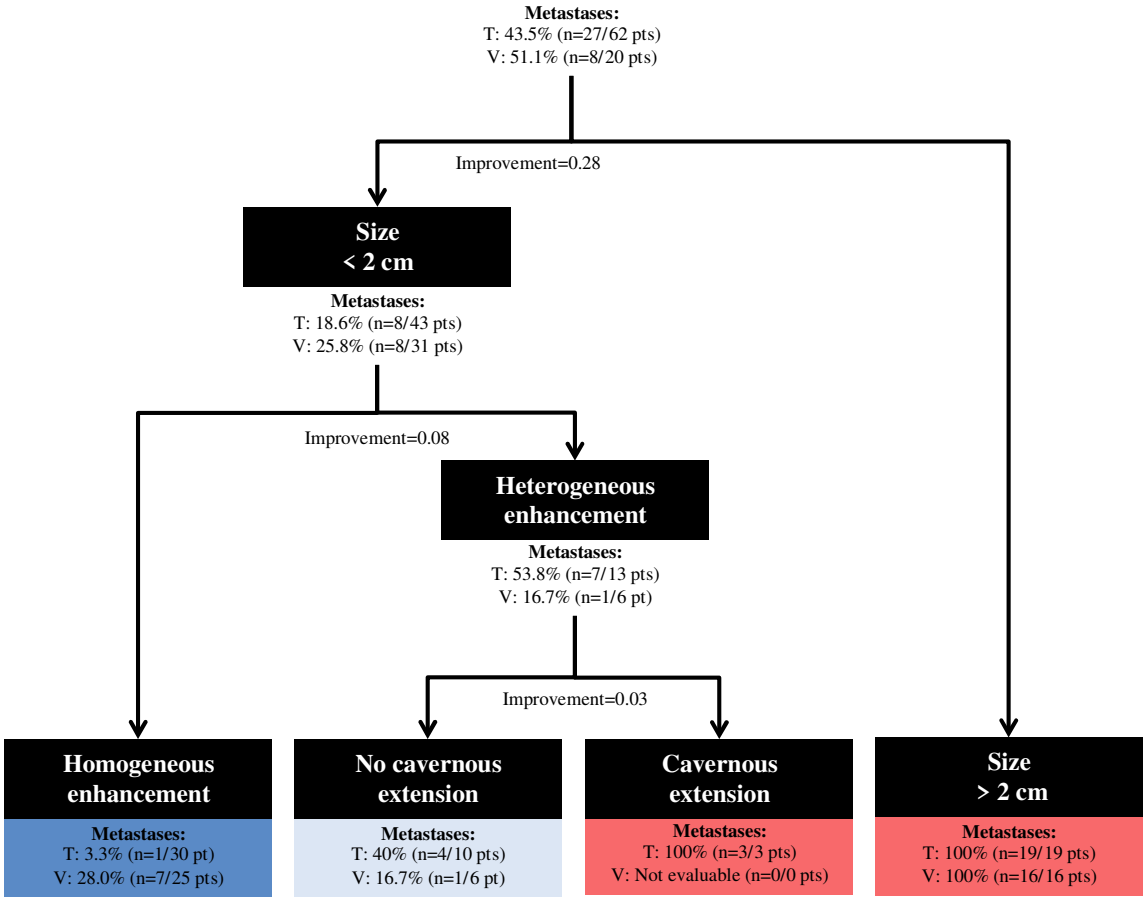

Risk	Signature	Diagnosis
Low-risk	0%	100 % Hypophysitis
	10%	90 % Hypophysitis
	20%	80 % Hypophysitis
	30%	70 % Hypophysitis
	40%	60 % Hypophysitis
	50%	Indeterminate
High-risk	60%	60 % Metastases
	70%	70 % Metastases
	80%	80 % Metastases
	90%	90 % Metastases
	100%	100% Metastases

Figure 4 : **AUC of the model for the diagnosis of pituitary hypophysitis.**

The ROC curve is represented in the overall population and reached similar performance in both the training set with AUC=0.91 (0.82, 1.00), $P<10^{-8}$, and in the validation set with AUC=0.94 (0.80, 1.00), P=0.001.

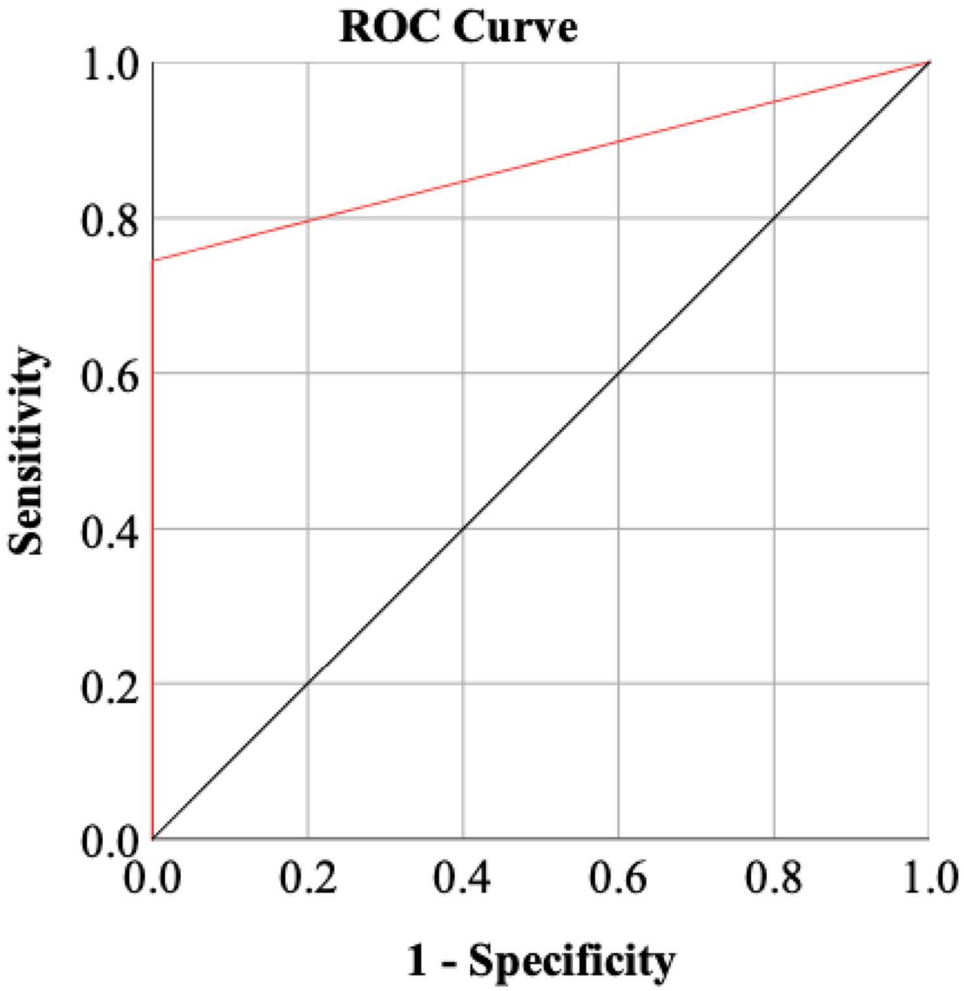

Table 1a: **Hypophysitis**

Study and patient characteristics. Abbreviations: NA = data not available; RCC = renal cell carcinoma; NSCLC = non-small cell lung cancer; SCC = squamous cell carcinoma; SCLC = small cell lung cancer; NET = neuroendocrine tumor, NE = neuroendocrine; HCC = hepatocellular carcinoma

Author	Year	Country	n	Cancer type	Age	Modality	Treatment type
Van der Hiel et al	2013	Netherlands	1	Melanoma	77	PET/CT	Ipilimumab
Blansfield et al	2005	United States	8	Melanoma, RCC	49 (31-61)	MR	Ipilimumab
Albarel et al	2014	France	15	Melanoma	55 (39-80)	MR	Ipilimumab
Araujo et al	2015	Brazil	1	Melanoma	60	MR	Ipilimumab
Carpenter et al	2009	United States	3	Melanoma	53 (44-70)	MR	Ipilimumab
Chang et al	2017	United States	1	Melanoma	77	MR	Ipilimumab+Nivolumab
Chodakiewitz et al	2014	United States	3	Melanoma	58 (45-65)	MR	Ipilimumab
Dillard et al	2009	United States	2	Prostate	59 (50-67)	MR	Ipilimumab
Hassanzadeh et al	2017	United States	1	Melanoma	64	MR	Ipilimumab
Johnson et al	2015	United States	1	Melanoma	60	MR	Ipilimumab
Juszczak et al	2012	United Kingdom	1	Melanoma	54	MR	Ipilimumab
Kaehler et al	2009	United Kingdom	1	Melanoma	60	MR	Ipilimumab
Kanie et al	2017	Japan	2	NSCLC	65 (61-69)	MR	Atezolizumab
Mahzari et al	2015	Canada	4	Melanoma	62 (54-80)	MR	Ipilimumab
Majchel et al	2015	United states	1	Melanoma	31	MR	Ipilimumab
Marlier et al	2014	Belgium	4	Melanoma	62 (31-81)	MR	Ipilimumab
Mekki et al	2018	France	3	NSCLC, RCC	59 (53-65)	MR	Nivolumab
Gunawan et al	2018	Australia	1	Melanoma	52	MR	Ipilimumab+Nivolumab
Ohara et al	2018	Japan	1	Oesophagus (SCC)	63	MR	Nivolumab
Okano et al	2016	Japan	1	Melanoma	50	MR	Nivolumab
Valecha et al	2017	United states	1	SCLC	58	MR	Ipilimumab+Nivolumab
Wachsmann et al	2016	United states	1	Melanoma	62	PET/CT	Ipilimumab
Wallace et al	2018	United states	1	Melanoma	49	MR	Ipilimumab
Arvinder et al	2017	United States	1	Melanoma	34	MR	Ipilimumab
Iqbal et al	2016	United Kingdom	1	Melanoma	65	MR	Ipilimumab

Table 1b: **Pituitary metastases**

Author	Year	Country	n	Cancer type	Age	Modality
Al-Aridi et al	2013	United States	1	NSCLC	-	MR
Dutta et al	2011	India	4	NSCLC	51 (39-60)	MR
Bhatoe et al	2008	India	1	Medullary thyroid	38	MR
Ersoy et al	2007	Turkey	1	Breast	55	PET/CT
Fridley et al	2011	United States	1	SCLC	56	MR
Goglia et al	2007	Italy	1	NET	69	MR
Golkowski et al	2007	Poland	2	Breast,RCC	49 (46-52)	MR
Gopan et al	2007	United States	5	RCC	60 (51-67)	MR
He et al	2014	United States	1	HCC	49	MR
Kam et al	2015	Australia	1	Breast	63	MR
Karamouzis et al	2003	Greece	1	HCC	59	MR
Ko et al	1994	China	1	Lung	67	MR
Koshiyama et al	1992	Japan	1	RCC	57	MR
Lin et al	2008	China	1	Breast	37	MR
Masui et al	2013	Japan	1	Melanoma	68	MR
Ozturk et al	2013	Turkey	1	Colorectal	46	MR
Peppa et al	2009	Greece	1	Breast	52	MR
Piedra et al	2004	United States	1	Breast	58	MR
Riemenschneider et al	2009	Germany	1	Prostate	64	MR
Siqueira et al	2015	Brazil	1	Lung NE	64	MR
Williams et al	2008	United States	1	Medullary thyroid	23	MR
Ratti et al	2013	Italy	1	Rectal	54	MR
Stovanovic et al	2012	Serbia	1	Papillary thyroid	67	MR
Beckett et al	1998	United Kingdom	1	RCC	56	MR
Moreno-Perez et al	2007	Spain	1	HCC	65	MR
Agarwal et al	2014	India	1	NSCLC	52	PET/CT, MR
Barbaro et al	2012	Italy	2	Papillary thyroid	64 (63-65)	MR
Kurkjianet al	2005	United Kingdom	2	Breast	51 (47-54)	MR
Santarpia et al	2009	United States	1	Medullary thyroid	23	MR
Wendel et al	2017	France	1	RCC	61	MR
Feletti et al	2010	Italy	1	Merkel	65	MR
Kim YH et al	2012	South Korea	1	Breast	65	MR
Chu et al	2016	China	1	Breast	60	MR
Kanayama et al	2005	Japan	1	Thymoma	80	MR
Souza mota et al	2018	Brazil	1	Follicular thyroid	58	MR
Rajput et al	2006	India	1	NSCLC	51	MR
Bisof et al	2008	Croatia	1	RCC	49	MR
Hsiao et al	2011	China	1	NSCLC	56	MR
Lim et al	2015	Singapore	2	Thyroid	58 (50-65)	MR
Castlekirszbaum et al	2018	Australia	12	Breast, oesophagus, NSCLC, SCLC, colorectal, melanoma, plasmocytoma	63 (30-87)	MR

Table 2: **Immune-related hypophysitis versus pituitary metastases**

	Hypophysitis	PM
Pituitary enlargment	n = 53/59 (89.%)	n = 62/62 (100%)
Homogenous enhancement	n = 31/49 (63.3%)	n = 8/46 (17.4%)
Heterogenous enhancement	n = 18/49 (36.7%)	n = 38/46 (82.6%)
Increased stalk thickness	n = 29/49 (59.2%)	n = 16/58 (27.6%)
Suprasellar extension	n = 35/59 (59.3%)	n = 57/62 (91.9%)
Cavernous extension	n = 0/59 (0%)	n = 31/61 (50.8%)
Size >2cm	n = 0/59 (0%)	n = 45/61 (73.8%)
18FDGPET hypermetabolism	n = 2/2 (100%)	n = 2/2 (100%)
Headache	n = 42/60 (70%)	n = 41/61 (67.2%)
Hypopituitarism	n = 56/60 (93.3%)	n = 50/59 (84.7%)
Diabetes insipidus	n = 3/60 (5%)	n = 26/52 (50%)

Table 3. **Sensitivity and accuracy of clinical features and imaging features.**

The machine learning algorithm was designed to maximize the sensitivity for the detection of pituitary metastases, while maintaining accuracy. The values and 95% confidence intervals listed below demonstrate that the algorithm exceeded the performance of any individual feature.

	Clinical features (all pts)			Imaging features (all pts)						Signature subset (complete dataset)	
	Headache	Hypopituitarism	Diabetes Insipidus	Pituitary enlargement	Heterogenous enhancement	Stalk thickened	Cavernous extension	Suprasellar extension	Size >2cm	Signature	Size >2cm
Total	121	119	112	121	95	107	120	121	110	82	82
Positive in PM	41	50	26	62	38	16	31	57	45	28	25
Positive in hypophysitis	42	56	3	53	18	29	0	35	0	0	0
Negative in PM	20	9	26	0	8	42	30	5	6	7	10
Negative in hypophysitis	18	4	57	6	31	20	59	24	59	47	47
Sensitivity	0.67 (0.55:0.78)	0.85 (0.73:0.92)	0.50 (0.37:0.63)	1.00 (1.00:1.00)	0.83 (0.72:0.94)	0.28 (0.16:0.39)	0.51 (0.38:0.63)	0.92 (0.85:0.99)	0.88 (0.79:0.97)	0.80 (0.67:0.93)	0.71 (0.56:0.86)
Specificity	0.30 (0.20:0.43)	0.07 (0.02:0.17)	0.95 (0.86:0,99)	0.10 (0.02:0.18)	0.63 (0.50:0.77)	0.41 (0.27:0.55)	1.00 (1.00:1.00)	0.41 (0.28:0.53)	1.00 (1.00:1.00)	1.00 (1.00:1.00)	1.00 (1.00:1.00)
False positive rate	0.70 (0.59:0.81)	0.93 (0.87:0.99)	0.05 (0.00:0.10)	0.90 (0.82:0.98)	0.37 (0.23:0.50)	0.59 (0.45:0.73)	0.00 (0.00:0.00)	0.59 (0.47:0.72)	0.00 (0.00:0.00)	0.00 (0.00:0.00)	0.00 (0.00:0.00)
False negative rate	0.33 (0.21:0.44)	0.15 (0.06:0.24)	0.50 (0.37:0.63)	0.00 (0.00:0.00)	0.17 (0.06:0.029)	0.72 (0.61:0.84)	0.49 (0.37:0.60)	0.08 (0.01:0.18)	0.12 (0.03:0.20)	0.20 (0.07:0.31)	0.28 (0.14:0.40)
Pred value positive	0.49 (0.39:0.60)	0.47 (0.38:0.57)	0.90 (0.79:1.00)	0.54 (0.45:0.63)	0.68 (0.56:0.80)	0.36 (0.22:0.50)	1.00 (1.00:1.00)	0.62 (0.52:0.72)	1.00 (1.00:1.00)	1.00 (1.00:1.00)	1.00 (1.00:1.00)
Pred value negative	0.47 (0.32:0.63)	0.31 (0.06:0.60)	0.69 (0.59:0.79)	1.00 (1.00:1.00)	0.79 (0.67:0.92)	0.32 (0.21:0.44)	0.66 (0.56:0.76)	0.83 (0.69:0.97)	0.91 (0.84:0.98)	0.87 (0.78:0.96)	0.82 (0.73:0.92)
Overall accuracy	0.50 (0.42:0.59)	0.50 (0.41:0.59)	0.46 (0.37:0.56)	0.56 (0.47:0.65)	0.73 (0.64:0.82)	0.34 (0.25:0.43)	0.75 (0.67:0.83)	0.67 (0.59:0.75)	0.95 (0.90:0.99)	0.91 (0.85:0.98)	0.88 (0.81:0.95)

Supplemental table

Median week of immune-related hypophysitis onset stratified by oncological response to the ICB

Best Overall Response	n	Median week (range)
PD	6	12 (6-18)
SD	5	21 (9-56)
PR	10	13.5 (3-34)
CR	4	6 (4-12)
Unknown	35	9 (3-28)
Overall	60	10.5 (3-56)